

Self-organized electronic superlattices in layered materials

Carmine Ortix,¹ Carlo Di Castro,² and José Lorenzana²

¹*Institute for Theoretical Solid State Physics, IFW Dresden, D01171 Dresden, Germany*

²*ISC-CNR and Dipartimento di Fisica, Università di Roma "La Sapienza", Piazzale Aldo Moro 2, 00185 Roma, Italy.*

We show that in layered systems with electronic phase separation tendency, the long-range Coulomb interaction can drive the spontaneous formation of unidirectional superlattices of electronic charge in a completely homogeneous crystalline background. In this self-organized electronic heterostructure, the ratio among the number of crystalline planes in the minority and majority electronic phases corresponds to Farey fractions with the superlattice period controlled by the background charge density and the frustrating Coulomb interaction strength. The phase diagram displays Arnold tongues obeying a modified Farey tree hierarchy and a devil's staircase typical of systems with frustration among different scales. We further discuss the competition of these electronic superlattices, recently observed in iron-based superconductors and mixed valence compounds, with in-plane electronically modulated phases.

PACS numbers: 73.21.Cd, 71.10.Hf, 64.75.Jk, 64.75.-g

Domain pattern formation is a beautiful example of cooperative behavior in a variety of systems with competing interactions on different length scales [1]. In strongly correlated electronic systems, electronic charge modulated phases are center stage with complex phenomena as colossal magnetoresistance [2–4], magnetoelectric effects [5], spin-Peierls-like behavior [6] and high-temperature superconductivity in cuprates [7–16] and iron-based superconductors [17–19]. In most of these systems short-range electronic correlations can and do often drive a tendency towards phase separation in electron-rich and electron-poor phases. Unless the counterions are mobile, the appearance of a macroscopically electronic phase segregated state is prohibited by the long-range part of the Coulomb interaction. Henceforth, the system compromises by stabilizing electronic microemulsions of the competing phases [7–9, 20] in the form of bubbles and stripes in two-dimensional (2D) systems [21], and layers, rods and droplets in three-dimensional (3D) ones [22]. Irregularities leading to fractal-like interfaces [23] can be ascribed to a non-negligible role of quenched disorder possibly stabilizing glassy states.

It has been theoretically established [21] that the appearance of these charge textures is particularly favored in 2D systems and indeed this phenomenon has been observed in materials which share a strictly 2D or quasi-2D layered structure. In layered systems, however, electronic phase separation tendencies can potentially lead to a phase segregated state consisting of alternating uniformly charged electron-rich and electron-poor crystalline planes [24] (hereafter the 1/1 structure) recently observed in the mixed valence compound LuFe_2O_4 [5]. The questions remain whether larger period phase segregated states of the same kind can be spontaneously stabilized and how the appearance of these electronic heterostructures competes with the formation of electronic microemulsions within the crystal planes. In this Letter, we show that when the frustrating Coulomb energy cost is small

compared to the phase-separation energy gain, a layered system self-organizes in unidirectional superlattices of electronic charge whose period depends on the average charge. The ensuing phase diagram from the homogeneous phase to the inhomogeneous one is characterized by Arnold tongues [25] obeying a modified Farey tree construction and a devil's staircase analogous to dynamical systems with competing frequencies [26] and solid-state structures with frustration among different scales [6].

To illustrate the emergence of electronically charged superlattices, we consider a layered system in which the coarse grained electronic free energy can be expressed phenomenologically as a Landau expansion in powers of an electronic charge density order parameter [22] $\phi_l(\mathbf{r})$,

$$\mathcal{F}_\phi = \sum_l \int [\phi_l(\mathbf{r})^2 - 1]^2 + |\nabla \phi_l(\mathbf{r})|^2 d\mathbf{r} + \sum_{l,l'} \frac{Q^2}{2} \int \frac{[\phi_l(\mathbf{r}) - \bar{\phi}][\phi_{l'}(\mathbf{r}') - \bar{\phi}]}{\sqrt{(\mathbf{r} - \mathbf{r}')^2 + a_3^2(l - l')^2}} d\mathbf{r} d\mathbf{r}', \quad (1)$$

where l is a layer index while \mathbf{r} is a two-dimensional intralayer position vector (measured in units of the in-plane bare correlation length ξ). The first term has a double well form favoring phase separation in the absence of the Coulomb interaction. Energies are measured in units of the barrier height whereas densities are in units such that in each layer $\phi_l(\mathbf{r}) = \pm 1$ represent the ideal densities n_+^0, n_-^0 of the electron rich and electron poor phases. More precisely, the physical electron areal density per plane l is $n_l(\mathbf{r}) = (n_+^0 + n_-^0)/2 + \phi_l(\mathbf{r})(n_+^0 - n_-^0)/2$. The second term in Eq. 1 accounts for short range surface energy effects. We assume very weak short-range interlayer couplings, as it is the case in many layered materials, and thus neglect the associated energy cost to create electronic domain walls in the stacking direction. The third term is the Coulomb energy, frustrating macroscopic phase separation, with a_3 as the spacing among the layers and Q^2 parameterizing the strength of

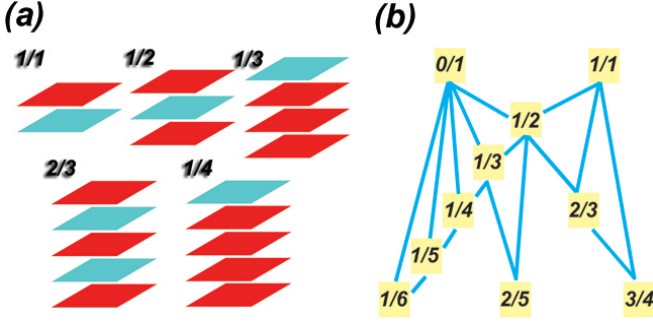


FIG. 1: (a) Sketch of the lowest period electronic heterostructures. (b) Schematics of the modified Farey tree construction. Each fraction p/q is generated by its ancestors p_a/q_a and p_b/q_b as $p/q = (p_a + p_b)/(q_a + q_b)$.

Coulomb frustration with respect to the barrier height of the double-well. Charge neutrality is guaranteed assuming a completely rigid ionic background of positive charge $-\bar{\phi}$ with $\sum_l \int \phi_l(\mathbf{r}) d\mathbf{r} = \bar{\phi} \sum_l \int d\mathbf{r}$. Hereafter we will refer to $\bar{\phi}$ as the global density. The ideal electron rich and electron poor physical densities $n_{+,-}^0$, as well as any other parameter in the model, are determined by control parameters like pressure, temperature, doping, etc. For example we expect $Q^2 \sim 1/(T^* - T)$ below a temperature T^* where thermodynamic phase separation would start in the absence of the stabilizing effect of the long-range Coulomb interaction.

We first consider the 1/1 structure with charge distribution [24], $\phi_l = \bar{\phi} + \delta\phi e^{i\pi l}$. The difference of free energy density among this modulated phase and the homogeneous one [see Supplemental Material] takes the form $\delta f = \alpha(Q, \bar{\phi}) \delta\phi^2 + \beta \delta\phi^4$ with $\alpha(Q, \bar{\phi})$ vanishing along a Gaussian second order transition line, $Q_G^{1/1} = 2[(1 - 3\bar{\phi}^2)/\pi a_3]^{1/2}$. As Q approaches $Q_G^{1/1}$ from above, the homogeneous phase is thus unstable toward a charge modulated phase. This second-order phase transition cannot survive in the $Q \rightarrow 0$ limit since it predicts a modulated phase for $|\bar{\phi}| < 1/\sqrt{3}$, in disagreement with macroscopic phase separation that instead secures an inhomogeneous phase in the larger range $|\bar{\phi}| < 1$. The way out of this discrepancy consists in considering inhomogeneous states with the electronic charge density modulated again along the stacking direction but with larger period arrangements. These can be identified by setting $Q = 0$ at first. The Maxwell construction predicts an inhomogeneous state with $\mathcal{F}_\phi = 0$ where the density in the layers $\phi_l = \pm 1$ and the ratio between the total number of layers in the minority and the majority phase is $(1 - |\bar{\phi}|)/(1 + |\bar{\phi}|)$. In our model this does not uniquely fix the inhomogeneous state: due to the absence of stiffness in the staking direction, there is a macroscopic degeneracy of different states fulfilling the Maxwell construction. This degeneracy is lifted once even infinitesimally small values of Q are introduced. The

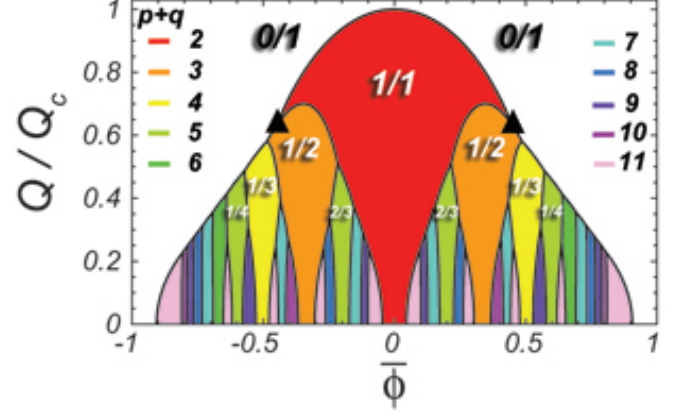


FIG. 2: Phase diagram in the uniform density approximation for $a_3 \leq \sqrt{6}$. The colors encode the periodicity $p + q$ of superlattices. The ▲ indicate the triple points separating a second-order transition line (above) from a first-order one (below). The strength of the Coulomb interaction has been measured in units of $Q_c = 2/\sqrt{\pi a_3}$. The appearance of the larger periodicity tongues goes at the expense of the lower periodicity tongues which acquire a funnel shape. We have restricted to structures with $p + q \leq 11$. Allowing for arbitrary periodicities would shrink the lower part of the funnel to one point.

long-range Coulomb interaction indeed selects the inhomogeneous states minimizing the periodicity while concomitantly maximizing the distance among the electronic domain walls within one period. This leads to uniquely defined superlattices of electronic charge [c.f. Fig.1(a) for a sketch of the lowest period arrangements] where in one period made of $p+q$ layers the ratio among the number of layers (p) in the minority phase and the number of layers (q) in the majority phase realizes the series of Farey fractions $p/q = (1 - |\bar{\phi}|)/(1 + |\bar{\phi}|)$ determined by changing the global density from $\bar{\phi} \equiv \pm 1$ (the 0/1 homogeneous phase) to $\bar{\phi} = 0$ (the 1/1 modulated phase).

The complete devil's staircase with all possible rational values of p/q obtained by varying the average density occurs only in the $Q \rightarrow 0$ limit. For finite Q , the electronically charged superlattices of largest lateral dimension are progressively suppressed as Q increases. To show this, we employ a uniform density approximation and assume that the charge density order parameters in the p minority phase crystalline planes and the q majority phase crystalline planes take constant values ϕ_- and ϕ_+ respectively. The constraint of charge neutrality yields $p\phi_- + q\phi_+ = (p + q)\bar{\phi}$. The finite Coulomb energy can be then expressed in terms of the electric field among two consecutive layers E_l whose discontinuity at the l th layer is related to the local charge density by $E_l - E_{l-1} = 4\pi(\phi_l - \bar{\phi})$ where ϕ_l is uniquely determined by the spatial arrangement of the phase minority and phase majority layers in one period. The difference of

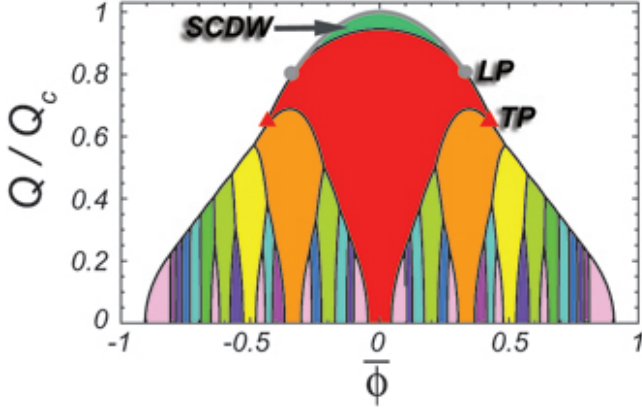


FIG. 3: Phase diagram including in-plane electronic microemulsions for a layered system with layer spacing $a_3 = 3\xi$. The strength of the Coulomb interaction has been measured in units of the maximum coupling strength $Q_c = 0.6623\dots$. The phase diagram displays two symmetric Lifshitz points (LP) and additional triple points (TP) at lower couplings.

free energy density among a modulated phase and the homogeneous one then takes the form

$$\delta f(p, q) = \frac{p}{q} [-2 + 6\bar{\phi}^2] \delta\phi_-^2 + 4\bar{\phi} \frac{p}{q} \left(1 - \frac{p}{q}\right) \delta\phi_-^3 \quad (2)$$

$$+ \frac{p}{q} \left(1 - \frac{p}{q} + \frac{p^2}{q^2}\right) \delta\phi_-^4 + \frac{1}{p+q} \sum_{l=1}^{p+q} \frac{Q^2 a_3}{8\pi} E_l^2,$$

where p and q are coprimes and $\delta\phi_- = \phi_- - \bar{\phi}$. Fig. 2 shows the ensuing phase diagram in the $Q - \bar{\phi}$ plane obtained by minimizing Eq. 2 with respect to $\delta\phi_-$ and scanning for the most energetically favored modulated structure with maximum periodicity $p + q = 11$. It shows the appearance of the so-called Arnold tongues [25] with the largest tongue appearing for the $p/q = 1/1$ superlattice. We identify the hierarchy of Arnold tongues size to follow a modified Farey tree construction: the tongues corresponding to p/q rationals $\in [0, 1]$ appear by lowering Q with increasing values of $p + q$ (rather than q alone as in the usual Farey tree construction) according to the rule that the largest tongue among p/q and p'/q' is $(p + p')/(q + q')$ [c.f. Fig.1(b) for the sequence of the modified Farey tree construction]. We emphasize that while, as discussed above, the transition from the homogeneous phase to the $1/1$ modulated state is second-order, the onset of inhomogeneous structures with $p + q > 2$ is first-order thereby leading to the appearance of a triple point in the phase diagram for the coexistence of the $0/1$, $1/1$ and $1/2$ phases $\{\bar{\phi}_T, Q_T\} = \{1/\sqrt{5}, \sqrt{8/(5\pi a_3)}\}$ determined by $\min_{\delta\phi_-} \delta f(1, 1) \equiv \min_{\delta\phi_-} \delta f(1, 2) \equiv 0$. By decreasing the frustration strength additional triple points are found for the coexistence of the $0/1$, $1/q$, $1/(q + 1)$ phases.

This, however, is not yet the end of the story. The

Coulomb cost associated to the formation of a generic superlattice of electronic charge is indeed $\propto a_3$ [c.f. Eq. 2] as it can be intuitively understood by considering two subsequent layers of the coexisting phases as a capacitance with $C \propto a_3^{-1}$ and Coulomb energy $E_c \propto C^{-1}$. It is then conceivable that by increasing the layer stacking distance the appearance of in-plane electronic microemulsions can preempt the formation of the electronic heterostructures discussed so far. This indeed occurs for $a_3 \geq \sqrt{6}$ [c.f. Supplemental Material for a detailed derivation]. To illustrate this point, we allow also for in-plane electronic charge density modulations. For a generic periodic texture, the electronic charge density can be expanded in momentum space as $\phi_l(\mathbf{r}) = \bar{\phi} + \sum_{\mathbf{G}} \phi_{\mathbf{G},l} e^{i\mathbf{G} \cdot (\mathbf{r} + \mathbf{T}_l)}$ where the \mathbf{G} 's are intralayer reciprocal lattice wavevectors and the \mathbf{T}_l 's account for an in-plane translation of the corresponding Bravais lattice with respect to a reference layer. In analogy with bulk 2D systems [see Supplemental Material], we consider both triangular and unidirectional charge density order, reminiscent of the charge density wave states observed on the surface of the transition metal dichalcogenide NbSe₂ [27], and restrict, for simplicity, to the corresponding simplest sets of in-plane wavevectors of equal magnitude G_0 . The long-range part of the free energy functional Eq. 1 is then minimized for in-plane charge density modulations oriented along the same direction but shifted by a value that is commensurate with their period $2\pi/G_0$. Specifically, sinusoidal charge density waves are shifted by half of their period in adjacent layers ($\mathbf{T}_l = \{\pi l/G_0, 0\}$) whereas in-plane charge density modulations with triangular symmetry render a three-layer stacking periodic structure with the vector $\mathbf{T}_l = \{4\pi l/(3G_0), 0\}$ [see Supplemental Material]. The allowed \mathbf{G} 's and the amplitudes $\phi_{\mathbf{G},l}$ become independent of the layers index l , i.e. $\phi_{\mathbf{G},l} = \phi_{\mathbf{G}}$. Precisely as in isotropic 2D and 3D systems [22], the optimal wavevector magnitude G_0 is selected by the competition among the Coulomb interaction and the gradient squared term in the total free energy functional \mathcal{F}_ϕ .

Having these combined in-plane and out-of-plane charge density textures in our hands, we have then determined the phase diagram in the $Q - \bar{\phi}$ plane by continuously changing the interlayer spacing a_3 while taking concomitantly into account the electronically charged superlattices. As anticipated above, for small interlayer distances ($a_3 < \sqrt{6}$) [see Supplemental Material] in-plane charge density modulations are completely suppressed and the phase diagram of Fig. 2 holds. Increasing a_3 a region of in-plane unidirectional sinusoidal charge density modulations (SCDW) first appears in the phase diagram at strong coupling [c.f. Fig. 3]. The SCDW's amplitude vanishes along a Gaussian instability line $Q_g^{SCDW} = Q_c(a_3) f(\bar{\phi}, Q, a_3)$ where $Q_c(a_3)$ indicates the maximum coupling strength above which only homogeneous states are allowed. As Q is lowered, we

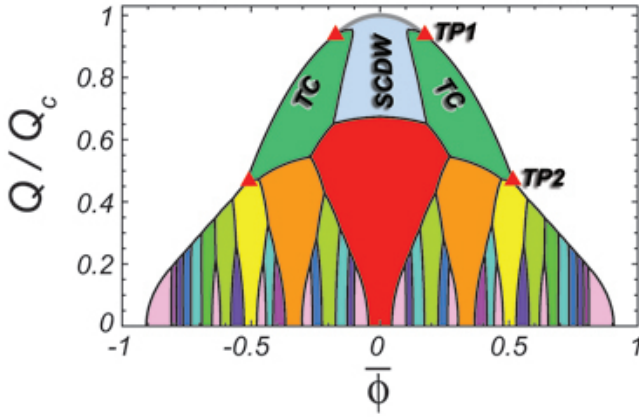


FIG. 4: Phase diagram for layer spacing $a_3 = 5\xi$. As before, the strength of the Coulomb interaction has been measured in units of the maximum coupling strength $Q_c = 0.5999\dots$. The phase diagram displays triple points from in-plane unidirectional to triangular modulated structures (TP1) and additional triple points (TP2) marking the disappearance of in-plane charge modulations.

find this second-order phase transition line to converge to the $1/1$ instability line $Q_G^{1/1}$. This, in turn, implies the appearance of two a_3 -dependent Lifshitz points $\{\bar{\phi}_L, Q_L\} = \left\{\pm\sqrt{1/3 - 2/a_3^2}, \sqrt{24/(\pi a_3^3)}\right\}$ where the period of the SCDWs diverges and their amplitude vanishes [see Fig.3 and Supplemental Material]. The presence of a second-order transition line to in-plane unidirectional charge density modulations is unique of anisotropic systems. Indeed it is not encountered in isotropic systems both in 2D [Supplementary Information] and 3D [22]. Such a feature is relevant for cuprates, where charge density wave ordering has been experimentally observed [12–15], as it allows for a second-order charge density wave quantum critical point relevant for superconductivity [7].

The occurrence of the Lifshitz points is lost as a_3 is increased further. The in-plane Gaussian instability line Q_g^{SCDW} indeed crosses a first-order transition line leading to in-plane triangular lattices of inhomogeneities at two new triple points $\{\pm\bar{\phi}_{TP1}, Q_{TP1}\}$ (with $Q_{TP1} > Q_L$) [see Fig.4] which are found to be exponentially close to the critical point of the phase diagram $\{\bar{\phi} = 0, Q_c(a_3)\}$ in the $a_3 \gg 1$ regime [Supplementary Information]. Two additional triple points (TP2 in Fig.4) at lower coupling strength mark the disappearance of in-plane charge density modulations. Independent of the a_3 value, the appearance of electronically charged superlattices is thus in general preserved at weak coupling [c.f. Figs. 3,4].

We have shown, in conclusion, that unidirectional superlattices of electronic charge can be spontaneously formed in layered materials with electronic phase separation tendencies. These phase segregated states realize an electronic structure analogous to the artificial unidirec-

tional superlattices built in conventional semiconductors by a periodic variation of composition during epitaxial growth [28] or in heterostructures of oxides [29]. The electronic superlattice period depends on the average charge and, within each period made of $p + q$ layers, the ratio p/q among the number of crystalline planes in the minority p and majority q electronic phases is governed by Farey fractions. By additionally varying the strength of Coulomb frustration – the ratio between the energy cost due to long-range forces and the typical phase separation energy gain – the phase diagram from the homogeneous phase to the inhomogeneous one displays Arnold tongues [25] with the largest tongues, ordered by size, appearing according to a modified Farey tree construction.

A long-period ($p + q \sim 10$) spontaneous electronic heterostructure, compatible with our proposal and consisting of alternating antiferromagnetic and superconducting planes, has been reported in iron-selenide superconductors [17, 18]. A short-period one ($p + q = 2$) has been observed on LuFe_2O_4 with bilayers playing the role of basic units. These observations suggest that this phenomenon might be more common than previously thought. Thus effects typical of heterostructures like Wannier-Stark quantization [30] and non-linear transport [31] may appear in these layered charge-ordered correlated systems with interesting perspectives for applications.

Acknowledgements – C.O. acknowledges support from FP7-NMP-2011-EU-Japan project (No.283204 SUPER-IRON). J.L. acknowledges support from the Italian Institute of Technology through the project NEWDFESCM.

-
- [1] M. Seul and D. Andelman, *Science* **267**, 476 (1995).
 - [2] T. Becker, C. Streng, Y. Luo, V. Moshnyaga, B. Damaschke, N. Shannon, and K. Samwer, *Phys. Rev. Lett.* **89**, 237203 (2002).
 - [3] L. Zhang, C. Israel, A. Biswas, R. L. Greene, and A. de Lozanne, *Science* **298**, 805 (2002).
 - [4] K. Lai, M. Nakamura, W. Kundhikanjana, M. Kawasaki, Y. Tokura, M. A. Kelly, and Z.-X. Shen, *Science* **329**, 190 (2010).
 - [5] J. de Groot, T. Mueller, R. A. Rosenberg, D. J. Keavney, Z. Islam, J.-W. Kim, and M. Angst, *Phys. Rev. Lett.* **108**, 187601 (2012).
 - [6] K. Ohwada, Y. Fujii, N. Takesue, M. Isobe, Y. Ueda, H. Nakao, Y. Wakabayashi, Y. Murakami, K. Ito, Y. Amemiya, H. Fujihisa, K. Aoki, T. Shobu, Y. Noda, and N. Ikeda, *Phys. Rev. Lett.* **87**, 086402 (2001).
 - [7] C. Castellani, C. Di Castro, and M. Grilli, *Phys. Rev. Lett.* **75**, 4650 (1995).
 - [8] V. Emery and S. Kivelson, *Physica C: Superconductivity* **209**, 597 (1993).
 - [9] U. Löw, V. J. Emery, K. Fabricius, and S. A. Kivelson, *Phys. Rev. Lett.* **72**, 1918 (1994).
 - [10] J. M. Tranquada, B. J. Sternlieb, J. D. Axe, Y. Nakamura, and S. Uchida, *Nature* **375**, 561 (1995).

- [11] P. Abbamonte, A. Rusydi, S. Smadici, G. D. Gu, G. A. Sawatzky, and D. L. Feng, *Nat Phys* **1**, 155 (2005).
- [12] J. Chang, E. Blackburn, A. T. Holmes, N. B. Christensen, J. Larsen, J. Mesot, R. Liang, D. A. Bonn, W. N. Hardy, A. Watenphul, M. v. Zimmermann, E. M. Forgan, and S. M. Hayden, *Nat Phys* **8**, 871 (2012).
- [13] G. Ghiringhelli, M. Le Tacon, M. Minola, S. Blanco-Canosa, C. Mazzoli, N. B. Brookes, G. M. De Luca, A. Frano, D. G. Hawthorn, F. He, T. Loew, M. M. Sala, D. C. Peets, M. Salluzzo, E. Schierle, R. Sutarto, G. A. Sawatzky, E. Weschke, B. Keimer, and L. Braicovich, *Science* **337**, 821 (2012).
- [14] R. Comin, A. Frano, M. M. Yee, Y. Yoshida, H. Eisaki, E. Schierle, E. Weschke, R. Sutarto, F. He, A. Soumyanarayanan, Y. He, M. Le Tacon, I. S. Elfimov, J. E. Hoffman, G. A. Sawatzky, B. Keimer, and A. Damascelli, *Science* **343**, 390 (2014).
- [15] E. H. da Silva Neto, P. Aynajian, A. Frano, R. Comin, E. Schierle, E. Weschke, A. Gyenis, J. Wen, J. Schneeloch, Z. Xu, S. Ono, G. Gu, M. Le Tacon, and A. Yazdani, *Science* **343**, 393 (2014).
- [16] K. M. Lang, V. Madhavan, J. E. Hoffman, E. W. Hudson, H. Eisaki, S. Uchida, and J. C. Davis, *Nature* **415**, 412 (2002).
- [17] A. Charnukha, A. Cvitkovic, T. Prokscha, D. Pröpper, N. Ocelic, A. Suter, Z. Salman, E. Morenzoni, J. Deisenhofer, V. Tsurkan, A. Loidl, B. Keimer, and A. V. Boris, *Phys. Rev. Lett.* **109**, 017003 (2012).
- [18] Y. Texier, J. Deisenhofer, V. Tsurkan, A. Loidl, D. S. Inosov, G. Friemel, and J. Bobroff, *Phys. Rev. Lett.* **108**, 237002 (2012).
- [19] J. T. Park, D. S. Inosov, C. Niedermayer, G. L. Sun, D. Haug, N. B. Christensen, R. Dinnebier, A. V. Boris, A. J. Drew, L. Schulz, T. Shapoval, U. Wolff, V. Neu, X. Yang, C. T. Lin, B. Keimer, and V. Hinkov, *Phys. Rev. Lett.* **102**, 117006 (2009).
- [20] Z. Nussinov, J. Rudnick, S. A. Kivelson, and L. N. Chayes, *Phys. Rev. Lett.* **83**, 472 (1999).
- [21] C. Ortix, J. Lorenzana, and C. Di Castro, *Phys. Rev. B* **73**, 245117 (2006).
- [22] C. Ortix, J. Lorenzana, and C. Di Castro, *Phys. Rev. Lett.* **100**, 246402 (2008).
- [23] M. Fäth, S. Freisem, A. A. Menovsky, Y. Tomioka, J. Aarts, and J. A. Mydosh, *Science* **285**, 1540 (1999).
- [24] B. V. Fine and T. Egami, *Phys. Rev. B* **77**, 014519 (2008).
- [25] H. G. Schuster and W. Just, *Deterministic chaos* (Wiley-VCH Verlag, Weinheim, 2005).
- [26] P. Bak, *Reports on Progress in Physics* **45**, 587 (1982).
- [27] A. Soumyanarayanan, M. M. Yee, Y. He, J. van Wezel, D. J. Rahn, K. Rossnagel, E. W. Hudson, M. R. Norman, and J. E. Hoffman, *Proceedings of the National Academy of Sciences* **110**, 1623 (2013).
- [28] L. Esaki and R. Tsu, *IBM J. Res. Develop.* **14**, 61 (1970).
- [29] A. Ohtomo, D. A. Muller, J. L. Grazul, and H. Y. Hwang, *Nature* **419**, 378 (2002).
- [30] J. Bleuse, G. Bastard, and P. Voisin, *Phys. Rev. Lett.* **60**, 220 (1988).
- [31] A. Wacker, *Physics Reports* **357**, 1 (2002).